Available online at www.sciencedirect.com
ScienceDirect
Dyes and Pigments 78 (2008) 199–206
DYES and PIGMENTS
www.elsevier.com/locate/dyepig

New azobenzene-containing polyurethanes: Post-functional strategy and second-order nonlinear optical properties

Zhichao Zhu [a], Qianqian Li [a], Qi Zeng [a], Zhong'an Li [a], Zhen Li [a,*], Jingui Qin [a], Cheng Ye [b]

[a] *Department of Chemistry, Wuhan University, Wuhan 430072, China*
[b] *Organic Solids Laboratories, Institute of Chemistry, The Chinese Academy of Sciences, Beijing 100080, China*

Received 26 September 2007; received in revised form 17 November 2007; accepted 21 November 2007
Available online 4 December 2007

Abstract

A new series of azobenzene-containing polyurethanes were prepared and post-azo coupling reactions were successfully used to modify the subtle structure of the azobenzene chromophore moieties. The polymers were characterized and their nonlinear optical properties were investigated by means of second harmonic generation processes. One of the polymers exhibited highest nonlinear optical effects ($d_{33} = 58.2$ pm/V), in which carbazolyl moieties were introduced to the chromophore groups as the isolation moieties. The results demonstrate the possibility of controlling the properties of polymers after the polymerization process.

Keywords: Nonlinear optical polyurethanes; Post-functionalization; Azo coupling reaction; Synthesis; Isolation groups; Structural modification

1. Introduction

Polymeric and monomeric azo-based materials have been paid great attentions in the past decades, due to their huge potential applications in high technology fields, such as waveguide switches, photomechanical systems, micropatterning, nonlinear optical (NLO) materials, and holographic memories. As the azobenzene compounds exhibit poor solubility in common solvents, they are usually introduced to polymer system as dopants (guest–host system) or as covalent construction blocks within the polymers (as the side chains or in the main chain). Generally, the latter is much better because of the avoidance of some disadvantages present in the guest–host systems, for example, the concentration limitation and bad compatibility of the azobenzene chromophores [1–23]. The frequently used synthetic route for the azobenzene-containing side-chain and main-chain polymers is the homo- or copolymerization of their corresponding monomers or to bond the azobenzene chromophores to the polymer backbone by the reaction between the azo moieties and the reactive groups of the polymers. However, in some special cases, this method does not work well. For example, in polyphosphazene system, it is very difficult to increase the concentration of Disperse Red 1 (DR1), a famous azo chromophore, as the side chains by the direct linkage reaction. Partially according to the literature [24], we improved the loading of DR1 to a large degree by using the post-azo coupling reaction [25]; the post-functional strategy also solved other problems encountered in direct linkage reactions [26–28]. Thus, the post-azo coupling reaction is an important and acceptable alternative for the preparation of azobenzene-containing polymers.

The azobenzene-containing polymers have been systematically studied as NLO materials, and recent researches demonstrate that, according to the site isolation principle [29,30], the introduction of some isolation groups to the azo chromophore moieties could dramatically improve the NLO effect of the resultant polymeric materials, by weakening the strong intermolecular dipole–dipole interactions between the highly polar azobenzene chromophore moieties in the polymeric system. Just this strong intermolecular electrostatic interaction

* Corresponding author. Tel.: +86 27 62254108; fax: +86 27 68756757.
E-mail address: lizhen@whu.edu.cn (Z. Li).

0143-7208/$ - see front matter © 2007 Elsevier Ltd. All rights reserved.
doi:10.1016/j.dyepig.2007.11.006

accounts for the fact that the NLO properties of the polymers are only enhanced several times even if the $\mu\beta$ values of chromophores have been improved by up to 250-fold [31–36].

Thus, based on our previous work [37–39], we wonder if it is possible to introduce additional reactive group to the azobenzene-containing polymers for further functionalization, for example, to introduce some isolation groups, during the post-azo coupling reaction of the polymers. If possible, we could control the subtle structure of the azobenzene chromophore moieties in polymers through polymer reactions, to adjust the properties of the resultant azobenzene-containing polymers. In the present article, with the above idea, we prepared a series of new azobenzene-containing polyurethanes, by applying the post-functional strategy (Scheme 1). The subtle structure of polymers **P3**–**P5** was adjusted by bonding different isolation moieties to the azobenzene groups, and the NLO effects of polymers were boosted from 34.6 pm/V of **P3** to much larger one (58.2 pm/V) of **P5**. Another special point is that **P2** could not be obtained from the direct polymerization of its corresponding monomers. Thus, our examples might give light on the syntheses of other polymers containing reactive groups for the further functionalization.

2. Experimental part

2.1. Materials

N,*N*-Dimethylformamide (DMF) was dried over and distilled from CaH_2 under an atmosphere of dry nitrogen. 2,4-Toluenediisocyanate (TDI) was purified by distillation under reduced pressure before use. 2-Amino-5-nitrophenol (**1**) was purchased from Acros. All other reagents were used as-received. *N*-Carbazolylacetic acid (**7**) was synthesized according to the methods reported in the literature [9]. Polyurethane **P1** was obtained from the copolymerization of 2,4-toluenediisocyanate (TDI) and *N*,*N*-(2-hydroxyethyl)aniline under similar polymerization conditions as reported previously [40–42].

2.2. Instrumentation

^{1}H NMR spectroscopic study was conducted with a Varian Mercury300 spectrometer using tetramethylsilane (TMS; $\delta = 0$ ppm) as internal standard. The Fourier transform infrared (FTIR) spectra were recorded on a Perkin–Elmer-2 spectrometer in the region of 4000–400 cm^{-1}. UV–vis spectra were obtained using a Shimadzu UV-2550 spectrometer. EI-MS spectra were recorded with a Finnigan PRACE mass spectrometer. Gel permeation chromatography (GPC) was used to determine the molecular weights of polymers. GPC analysis was performed on an Agilent 1100 series HPLC system and a G1362A refractive index detector. Polystyrene standards were used as calibration standards for GPC. THF was used as an eluent and the flow rate was 1.0 mL/min. Thermal analysis was performed on NETZSCH STA449C thermal analyzer at a heating rate of 10 °C/min in nitrogen at a flow rate of 50 cm^3/min for thermogravimetric analysis (TGA). The thermal transitions of the polymers were investigated using a METTLER differential scanning calorimeter DSC200PC under nitrogen at a scanning rate of 10 °C/min. The thickness

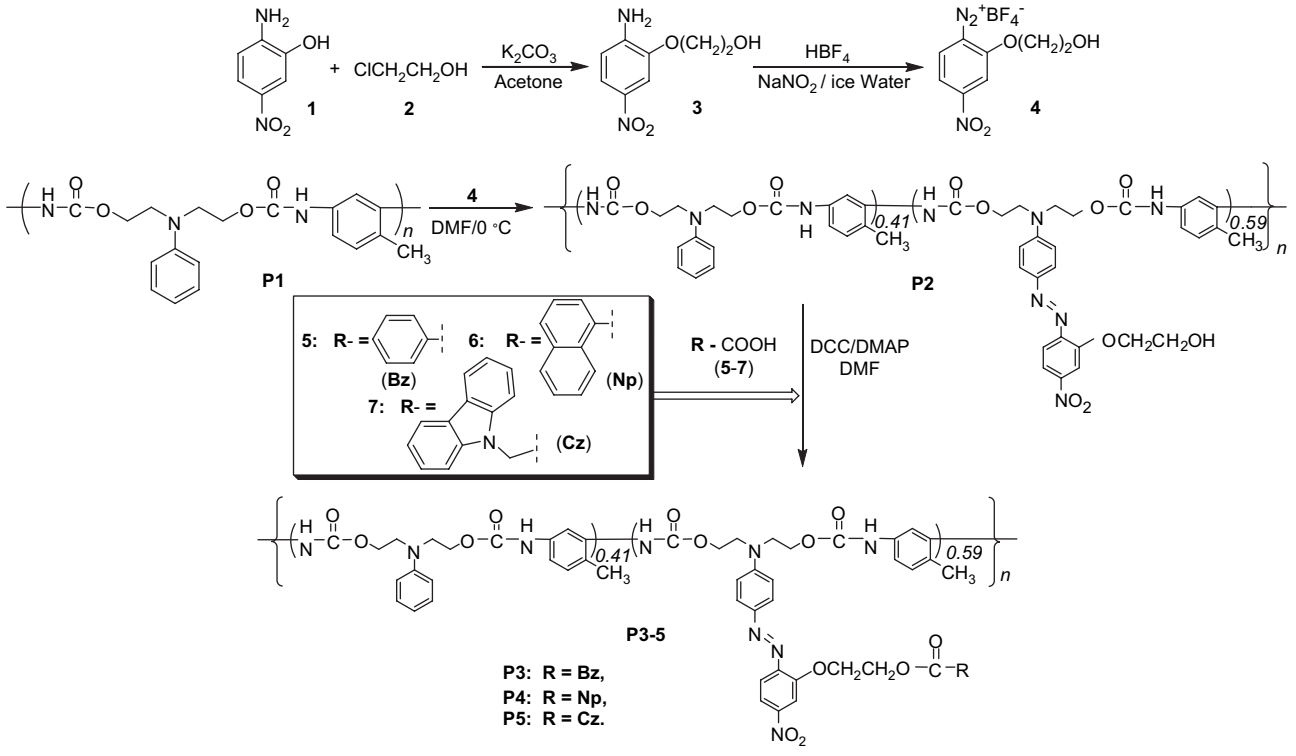

Scheme 1.

of the films was measured with an Ambios Technology XP-2 profilometer.

2.3. Synthesis of **3**

2-Chloroethanol (**2**) (0.8 g, 10 mmol) and potassium carbonate (2.8 g, 20 mmol) were added to the solution of **1** (1.54 g, 10 mmol) in acetone (77 mL) and the reaction mixture was refluxed at 60 °C for 43 h. After cooled to room temperature, the resultant mixture was filtered, and the solvent in the filtrate was removed under reduced pressure. The crude solid was further purified by column chromatography on silica gel using petroleum ether/ethyl acetate (1:2) as an eluent to yield the pure yellow product (1.37 g, 69.2%). Mp = 144–145 °C. ^{1}H NMR (acetone-d_6) δ (ppm): 3.94 (t, $J = 4.2$ Hz, 2H, $-OCH_2CH_2-$), 4.19 (t, $J = 4.5$ Hz, 2H, $-OCH_2CH_2-$), 6.75 (d, $J = 9.0$ Hz, 1H, ArH), 7.67 (s, 1H, ArH), 7.75 (d, $J = 8.7$ Hz, 1H, ArH). MS (EI), *m/z* [M^+]: 198.0, calcd. 198.1.

2.4. Synthesis of **4**

Compound **3** (1.98 g, 10 mmol) was dissolved in fluoroboric acid (40%, 4.5 mL) and then the solution was cooled to 0 °C. A solution of sodium nitrite (0.69 g, 10 mmol) in ice water (1.4 mL) was added dropwise. The resultant mixture was stirred at 0 °C for 1 h and then put into a refrigerator overnight. The white solid was filtered quickly and washed with cool ethanol and ether for several times. The solid was collected, and stored in the refrigerator (2.88 g, 97.0%).

2.5. Synthesis of **P2**

Polyurethane **P1** (0.96 g) was dissolved in DMF (7.5 mL) and then the resultant solution was cooled to 0 °C in an ice bath. Compound **4** (2.41 g) was added and the color of the solution changed to red immediately. After stirred for 12 h at 0 °C, excessive anhydrous potassium carbonate was added and the mixture was further stirred for half an hour before filtration. The residue was washed with THF and then the filtrate was collected. After THF was removed under reduced pressure, the red solution was added dropwise to methanol. The precipitate was collected and further purified by several precipitations from THF into methanol, and dried in a vacuum to a constant weight (1.37 g, 89.8%). $M_w = 82\,700$, $M_w/M_n = 1.32$ (GPC, DMF, polystyrene calibration). IR (thin film), ν (cm^{-1}): 1720 (C=O), 1339 ($-NO_2$). ^{1}H NMR (DMSO-d_6) δ (ppm): 2.05 ($-CH_3$), 3.76 ($-N-CH_2-$), 3.98 ($-O-CH_2-$ and $-CH_2OH$), 4.25 ($-CH_2OCO-$), 6.97–7.12 (ArH), 7.45–7.56 (ArH), 7.75–7.82 (ArH), 7.93 (ArH), 8.88–8.97 (–NH–), 9.61 (–NH–). UV–vis (DMF, 0.02 mg/mL): λ_{max} (nm): 485.

2.6. General procedure for the synthesis of **P3–P5**

Polymer **P2** (200 mg, 1.00 equiv) was dissolved in DMF (1.6 mL). Then a solution (1.6 mL) of compound **5** or **6** or **7** (5.00 equiv), 4-(*N*,*N*-dimethyl)aminopyridine (DMAP) (0.4 equiv) and dicyclohexylcarbodiimide (DCC) (5.00 equiv) was added. The resultant mixture was allowed to stir at room temperature for 72 h under nitrogen and then filtered to remove the insoluble solid. The filtrate was added dropwise to methanol to precipitate the polymer, which was further purified by several precipitations from THF into methanol, and dried in a vacuum to a constant weight.

Polymer **P3**: wine-red powder (150 mg, 66.5%). $M_w = 17\,700$, $M_w/M_n = 1.55$ (GPC, polystyrene calibration). IR (thin film), ν (cm^{-1}): 1722 (C=O), 1340 ($-NO_2$). ^{1}H NMR (DMSO-d_6) δ (ppm): 2.07 ($-CH_3$), 3.78 ($-N-CH_2-$), 4.27 ($-NCH_2CH_2-$), 4.63–4.68 ($-O-CH_2-$ and $-CH_2OCO-$), 6.88–6.90 (ArH), 7.05–7.16 (ArH), 7.40 (ArH), 7.52–7.56 (ArH), 7.69–7.71 (ArH), 7.84–7.93 (ArH), 8.02 (ArH), 8.92–9.01 (–NH–), 9.65 (–NH–). UV–vis (THF, 0.02 mg/mL): λ_{max} (nm): 471.

Polymer **P4**: wine-red powder (220 mg, 92.5%). $M_w = 15\,800$, $M_w/M_n = 1.56$ (GPC, polystyrene calibration). IR (thin film), ν (cm^{-1}): 1718 (C=O), 1340 ($-NO_2$). ^{1}H NMR (DMSO-d_6) δ (ppm): 2.04 ($-CH_3$), 3.58–3.70 ($-N-CH_2-$), 4.20 ($-NCH_2CH_2-$), 4.64–4.76 ($-O-CH_2-$ and $-CH_2OCO-$), 6.72–6.85 (ArH), 7.06–7.13 (ArH), 7.46–7.62 (ArH), 7.87 (ArH), 8.03 (ArH), 8.70 (ArH), 8.89–8.98 (–NH–), 9.62 (–NH–). UV–vis (THF, 0.02 mg/mL): λ_{max} (nm): 469.

Polymer **P5**: wine-red powder (232 mg, 92.4%). $M_w = 17\,670$, $M_w/M_n = 1.57$ (GPC, polystyrene calibration). IR (thin film), ν (cm^{-1}): 1730 (C=O), 1339 ($-NO_2$). ^{1}H NMR (DMSO-d_6) δ (ppm): 2.06 ($-CH_3$), 3.78 ($-N-CH_2-$), 4.26 ($-NCH_2CH_2-$), 4.48–4.55 ($-O-CH_2-$ and $-CH_2OCO-$), 5.29 ($-CH_2-$), 6.94 (ArH), 7.08–7.11 (ArH), 7.25 (ArH), 7.40–7.42 (ArH), 7.51 (ArH), 7.62–7.65 (ArH), 7.78–7.80 (ArH), 7.88–7.95 (ArH), 8.04–8.06 (ArH), 8.92–9.02 (–NH–), 9.66 (–NH–). UV–vis (THF, 0.02 mg/mL): λ_{max} (nm): 473.

2.7. Synthesis of compound **9**

Compound **3** (0.20 g, 1 mmol) was dissolved in a solution of 18% (wt) hydrochloride acid (2.2 mL). The mixture was cooled to 0 °C in an ice bath. A solution of sodium nitrite (0.069 g, 1 mmol) in 1 mL of water was added slowly and the mixture was stirred in the ice bath for 30 min. After this, the mixture was filtered to give a transparent solution. To this solution, *N*,*N*-(2-hydroxyethyl)aniline (**8**) (0.181 g, 1 mmol) in 1.3 mL of ethanol was added dropwise and the resultant mixture was stirred for 2 h in an ice bath. The crude product was precipitated out by neutralizing the reaction mixture with sodium bicarbonate solution, and further purified by recrystallization from THF to afford a dark red crystalline solid (0.31 g, 79.4%). Mp = 178–179 °C. ^{1}H NMR (DMSO-d_6) δ (ppm): 3.57 (s, br, 8H, $-NCH_2CH_2-$ and $-NCH_2CH_2-$), 3.80 (t, $J = 4.2$ Hz, 2H, $-OCH_2CH_2OH$), 4.28 (t, $J = 4.5$ Hz, 2H, $-OCH_2CH_2-$), 6.88 (d, $J = 9.0$ Hz, 2H, ArH), 7.61 (d, $J = 8.7$ Hz, 1H, ArH), 7.78 (d, $J = 8.7$ Hz, 2H, ArH), 7.88 (d, $J = 8.7$ Hz, 1H, ArH), 7.96 (s, br, 1H, ArH). ^{13}C NMR (DMSO-d_6) δ (ppm): 54.1, 58.9, 60.3, 72.4, 79.9, 110.5, 112.2, 117.1, 117.7, 126.6, 144.0, 147.3, 148.3, 152.6, 155.6. IR (thin film), ν (cm^{-1}): 1327 ($-NO_2$). MS

(EI), *m/z* [M^+]: 390.2, calcd. 390.2. UV–vis (DMF, 2.5×10^{-5} mol/L): λ_{max} (nm): 505.

2.8. Preparation of polymer thin films

The polymers were dissolved in THF (concentration ~3 wt%) and the solutions were filtered through syringe filters. Polymer films were spin-coated onto indium-tin-oxide (ITO)-coated glass substrates, which were cleaned by *N*,*N*-dimethylformamide, acetone, distilled water and THF sequentially in ultrasonic bath before use. Residual solvent was removed by heating the films in a vacuum oven at 40 °C.

2.9. NLO measurement of poled films

The second-order optical nonlinearity of the polymers was determined by in situ second harmonic generation (SHG) experiment using a closed temperature-controlled oven with optical windows and three needle electrodes. The films were kept at 45° to the incident beam and poled inside the oven, and the SHG intensity was monitored simultaneously. Poling conditions were as follows: temperature: different for each polymer (Table 1); voltage: 7.0 kV at the needle point; gap distance: 0.8 cm. The SHG measurements were carried out with an Nd:YAG laser operating at a 10 Hz repetition rate and an 8 ns pulse width at 1064 nm. A Y-cut quartz crystal served as the reference.

3. Results and discussion

3.1. Synthesis

The synthetic route is demonstrated in Scheme 1. Compound **3** was prepared under the similar reaction conditions as reported previously [43]. Then, this aniline was converted to its fluoroborate salt (**4**) smoothly as other benzenediazonium fluoroborates [44]. From two cheap commercial products, TDI and *N*,*N*-(2-hydroxyethyl)aniline, polyurethane **P1** was yielded in a large scale. Thus, the following polymers, **P2**–**P5**, could be derived from the same batch of **P1**, assuring their similar molecular weights for the comparison of their properties on the same level. Through post-azo coupling reaction, the structure of azobenzene was successfully constructed, while an additional hydroxyl group bonded to the side chain of **P2** simultaneously. Just by utilizing this newly introduced hydroxyl group, we could adjust the subtle structure of the chromophore moieties to some degree by the following ester formation between **P2** and different carboxylic acids. As shown in Scheme 1, benzoic acid (Bz), 1-naphthoic acid (Np) and *N*-carbazolylacetic acid (Cz) were selected as the isolation moieties to modify the azobenzene side chains of **P2**, as they could be easily obtained and with different bulk sizes. Thus, our approach to **P3**–**P5** comprised the post-polymerization azo coupling and ester formations, with the usage of the different reactive properties of aniline and hydroxyl groups. To the best of our knowledge, there are no reports from other groups about the combination of these two different reactions to functionalize polymers through polymer reactions.

All the post-functional polymer reactions were conducted under mild conditions, and the purification procedure was very simple. So, our examples demonstrate the synthetic flexibility of the post-functional strategy, especially the introduction of an additional reactive group to the side chain of polymers. By applying this post-functional strategy, we would like to design and synthesize other functional polymers inaccessible from the polymerization of their corresponding monomers. Further study is still under way in our lab.

3.2. Structural characterization

The polymers were well characterized. As shown in Fig. 1, in the IR spectrum of **P2**, a new strong absorption peak appeared at 1339 cm^{-1}, which was attributed to the absorption

Table 1
Polymerization results and characterization data

No.	Yield (%)	M_w [a]	M_w/M_n [a]	λ_{max} [b] (nm)	T_g [c] (°C)	T_d [d] (°C)	T [e] (°C)	d_{33} [f] (pm/V)
P1	90.3	17 400	1.79	291 (293)				
P2	89.8	[g]	[g]	471 (484)				
P3	66.5	17 700	1.55	471 (483)	107	270	113.5	34.6
P4	92.5	15 800	1.56	469 (486)	110	273	117.5	40.0
P5	92.4	17 670	1.57	473 (487)	136	258	126.3	58.2

[a] Determined by GPC in THF on the basis of polystyrene calibration.
[b] The maximum absorption wavelength of polymer solutions in THF, while the maximum absorption wavelength of their diluted solutions in DMF are given in the parentheses.
[c] Glass transition temperature (T_g) of polymers detected by the DSC analyses under nitrogen at a heating rate of 10 °C/min.
[d] The 5% weight loss temperature of polymers detected by the TGA analyses under nitrogen at a heating rate of 10 °C/min.
[e] The best poling temperature.
[f] Second harmonic generation (SHG) coefficient.
[g] Not obtained due to its poor solubility in THF.

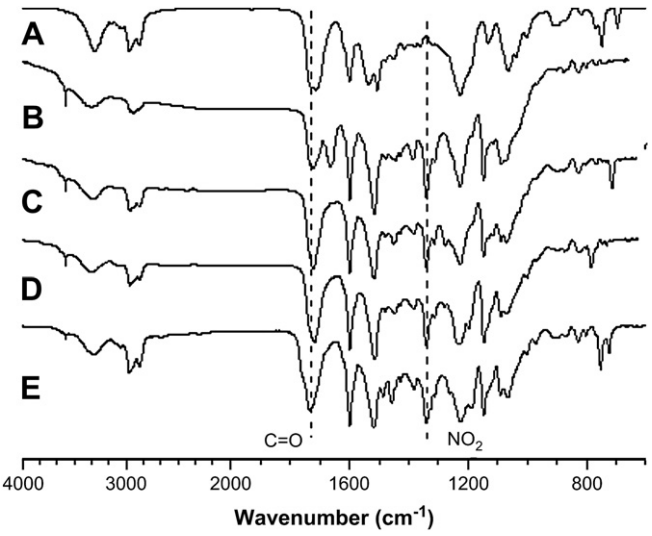

Fig. 1. IR spectra of polymers (A) **P1**, (B) **P2**, (C) **P3**, (D) **P4**, and (E) **P5**.

of the nitro groups, indicating that the post-azo coupling reaction was successful, and the structure of the azobenzene was constructed.

Polymers **P3**–**P5** were easily soluble in polar solvents, such as THF, DMF and DMSO, though **P2** exhibited poor solubility in THF (it could be dissolved in THF at low concentration). Similar to the case in the IR spectrum of **P2**, there was a new strong absorption peak with the maximum absorption wavelength at 471 nm (due to the $\pi-\pi^*$ transition of the nitro azo chromophore moieties), which further confirmed the successful attachment of azobenzene groups to the polymer backbone (Fig. 2). This absorption peak remained in **P3**–**P5**, though different isolation groups bonded to the chromophore moieties through the ester formation. This indicated that the push–pull structure of the formed azobenzene chromophore moieties was nearly unaffected by the attached isolation part. That is to say, the electronic properties of the chromophore groups in polymers remained nearly the same, no matter there were isolation moieties or not, or different ones. This result assured that the different NLO properties should be only caused by the different isolation moieties introduced, and we will discuss this point in detail later. The sharp peak at 291 nm in the spectrum of **P5** was ascribed to the absorption of the carbazolyl moieties.

From the UV–vis spectra, we could also determine the molar ratio of the azobenzene groups and the unreacted aniline moieties in **P2** accurately. A model compound (**9**, Scheme 2) was prepared from the normal azo coupling reaction. Then, a series of DMF solutions of **9** with concentration in the range of 1×10^{-5} mol/L to 4×10^{-5} mol/L were prepared, and a calibration curve was drawn from their absorption data at 505 nm in UV–vis spectra. The spectrum of a DMF solution of **P2**

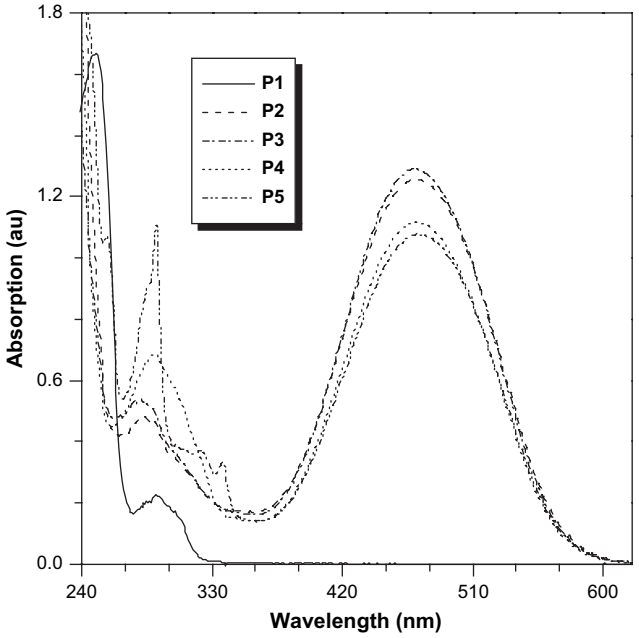

Fig. 2. UV–vis absorption spectra of THF solutions of polymers **P1**–**P5** (concentration: 0.02 mg/mL).

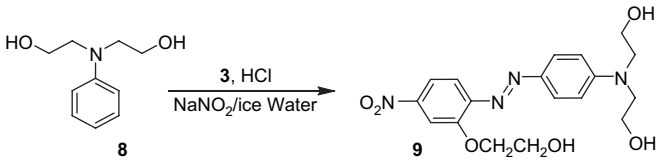

Scheme 2.

(0.02 mg/mL) was then measured. Using the calibration curve, the molar ratio of the azobenzene moieties in **P2** was calculated to be 0.59.

Also, the molar concentration of azobenzene moieties could be calculated from the ^{1}H NMR spectrum of **P2**. As shown in Fig. 3, after the post-azo coupling reaction, a new absorption peak appeared at 3.98 ppm, which should be ascribed to the ethylene groups between the two oxygen atoms, in addition to some other new peaks present at around 7.70 ppm. The molar ratio of the azobenzene moieties in **P2** was calculated to be 0.63, by comparing the integrations of signal peaks at 3.98 ppm (the ethylene groups) and 3.76 ppm (the alkyl protons linked to the nitrogen atoms in the main chain). This results was similar to that obtained in their UV–vis spectra.

In the ^{1}H NMR spectra of **P3**–**P5**, the chemical shifts were also consistent with the proposed structures as demonstrated in Scheme 1, and that of **P5** was selected as an example (Fig. 3C). Influenced by the linked carboxylic groups, the absorption peak of the ethylene groups between the two oxygen atoms shifted from 3.98 ppm to about 4.5 ppm and the original peak at 3.98 ppm disappeared completely, indicating that there was no unreacted hydroxyl groups present in **P5**. This case was further confirmed by analyzing the peak integrations of the methylene groups linked with the nitrogen atoms of carbazolyl moieties at 5.29 ppm, and the alkyl protons linked to the nitrogen atoms in the main chain at 3.76 ppm.

The molecular weights of polymers were determined by gel permeation chromatography (GPC), with THF as an eluent and polystyrene standards as calibration standards. All the results are summarized in Table 1. Polymers **P3**–**P5** possessed similar molecular weights and this would facilitate the

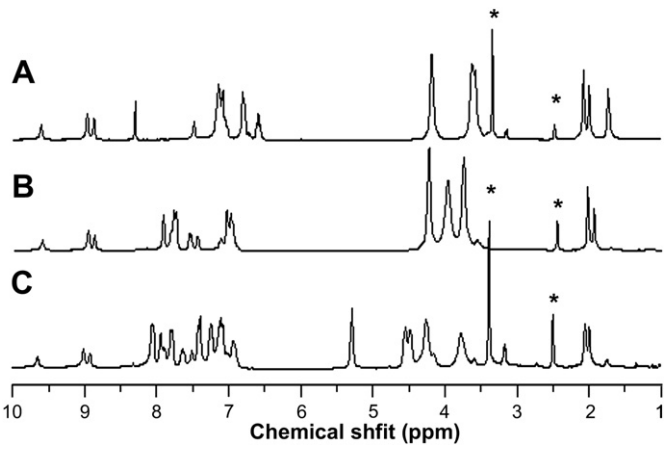

Fig. 3. ^{1}H NMR spectra of (A) **P1**, (B) **P2**, and (C) **P5** in dimethylsulfoxide-d_6. The solvent and water peaks are marked with asterisks (*).

comparison of their properties on the same level. Polymers **P3**–**P5** were thermolytically resistant, and exhibited nearly the same thermal stability. Their TGA thermograms are shown in Fig. 4, while the 5% weight loss temperatures of them is listed in Table 1. Also, by using a Setaram differential scanning calorimeter, the glass transition temperature (T_g) of the polymers was investigated (Table 1). Polymers **P3** and **P4** have a moderate T_g (~110 °C), and **P5** has a higher T_g of 136 °C, partially due to the strong secondary forces between polymer chains. The introduced bulky isolation groups (carbazolyl moieties) might also contribute to the higher T_g of **P5**.

3.3. NLO properties

The thin films of **P3**–**P5** were prepared to evaluate the NLO activity of the polymers, which was studied by investigating the second harmonic generation (SHG) processes characterized by d_{33}, an SHG coefficient. The method for the test of the SHG coefficients (d_{33}) for the poled films has been reported in our previous papers [45–49]. From the experimental data, the d_{33} values of **P3**–**P5** were calculated at 1064 nm fundamental wavelength (Table 1).

Although the three polymers contain the same NLO active chromophore moieties, they exhibit different d_{33} values, due to the different structures caused by the different isolation groups. As indicated by the similar maximum absorption observed in their UV–vis spectra, the linkage of the isolation spacers did not affect the electronic properties of the chromophore moieties. Thus, the different NLO properties of the polymers should be caused by the difference of the isolation groups, and especially related to their size. From **P3** to **P5**, the size of the isolation groups increased step by step, accordingly, the NLO effect increased from 34.6 pm/V of **P3** to 58.2 pm/V of **P5** (enhanced nearly 1.7 times). To see this trend more visually, Fig. 5 shows the comparison of the d_{33} values of the polymers (Curve A), using **P3** as the reference. Thus, the carbazolyl groups are the best isolation groups among the three polymers.

Since the introduction of different isolation groups would surely lead to the different molar weights of the obtained chromophores, we should consider the different molar concentrations of the active chromophore moieties in the polymers. According to the one-dimensional rigid orientation gas model [50],

$$d_{33} = \frac{1}{2} N \beta f^{2\omega} (f^{\omega})^2 \langle \cos^3 \theta \rangle \quad (1)$$

where N is the number density of the chromophore, β is its first hyperpolarizability, f is the local field factor, 2ω is the double frequency of the laser, ω is its fundamental frequency, and $\langle \cos^3 \theta \rangle$ is the average orientation factor of the poled film. As the active NLO chromophore moieties in **P3**–**P5** are the same, which should exhibit the same first hyperpolarizability (β), under identical experimental conditions, d_{33} should be proportional to the number density of the chromophore moieties in the polymers. Therefore, considering the active concentration of the chromophore moieties in the polymers, we could compare the results again with that of **P3** as the reference (Curve B, Fig. 5). The trend is nearly the same.

These results coincide well with the site isolation principle. In our case, the azobenzene moieties are highly polar groups with large dipole moments, leading to a centrosymmetric packing model in polymers due to the strong intermolecular dipole–dipole interactions. This status would surely make the poling-induced noncentrosymmetric alignment of azobenzene chromophores under electric field a daunting task and the

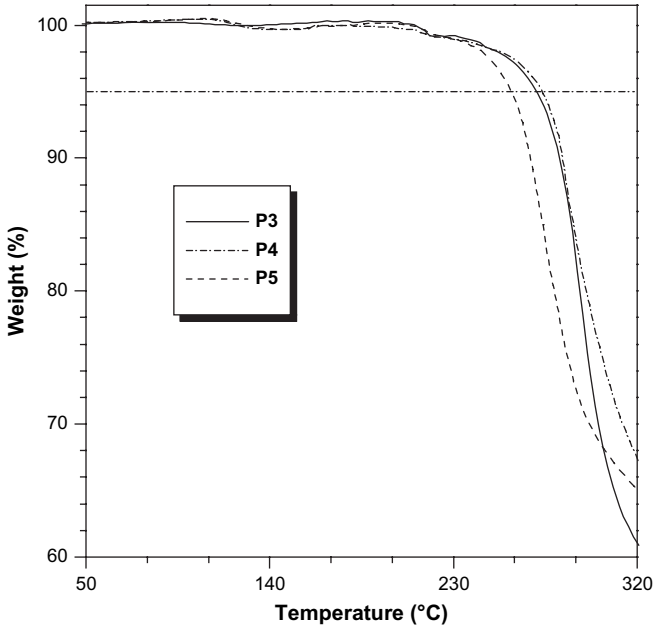

Fig. 4. TGA thermograms of **P3**–**P5** measured in nitrogen at a heating rate of 10 °C/min.

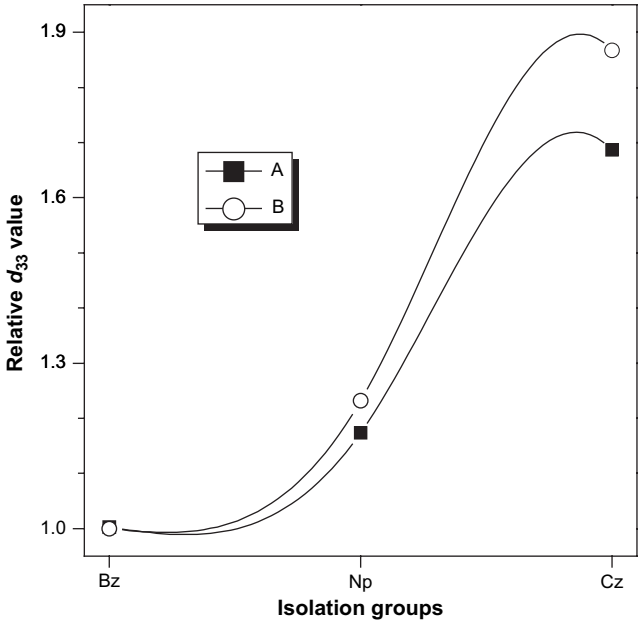

Fig. 5. (A) The comparison of the d_{33} values of the polymers **P3**–**P5**, (B) the comparison of the calculated d_{33} values, which were obtained by using the tested d_{33} values dividing the concentration of the active chromophore moieties of the polymers, using **P3** as a reference.

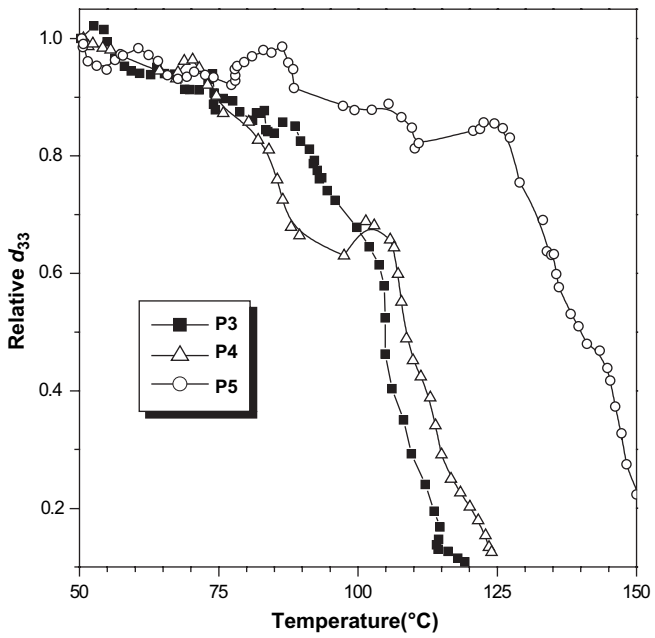

Fig. 6. Decays of SHG coefficient of **P3**–**P5** as a function of temperature.

strong dipole–dipole interactions could be weakened by the bonded isolation groups, due to the enlarged distance of the azobenzene chromophore moieties. As the biggest isolation group in the three ones, carbazolyl group could minimize the electronic interactions in a larger degree and this fact might account for the best NLO property of **P5**.

In comparison with that of **P3**, the macroscopic NLO effect of the same azobenzene chromophore moieties was boosted to 1.7 times higher in **P5**. This result demonstrates the positive effect of the introduced isolation group, and also indicates the importance of the usage of suitable isolation moieties. As the microscopic $\mu\beta$ value of the present azobenzene chromophore is relatively small, larger macroscopic NLO effects could be obtained if other better NLO chromophores with higher microscopic $\mu\beta$ value were used. Thus, our examples realize the possibility of modifying the NLO properties of polymers by adjusting the subtle structure of their contained NLO chromophore moieties through polymer reactions.

The dynamic thermal stabilities of the NLO activities of the polymers were investigated by the depoling experiment, in which the real time decays of their SHG signals are monitored as the poled films are heated from 45 °C to 150 °C in air at a rate of 4 °C/min. **P5** shows the best thermal stability with the onset temperature for decays in the d_{33} values at around 125 °C, possibly due to the presence of the large carbazolyl groups, which resulted in the relatively higher glass transition temperature in comparison with those of **P3** and **P4** (Fig. 6). Thus, the introduction of isolation groups not only benefits the NLO properties of the resultant materials, but also affects other behaviors related to their practical applications.

4. Conclusion

By applying post-functional strategy, new azobenzene-containing polyurethanes were prepared through polymer reactions (including post-polymerization azo coupling and esterization reactions) conveniently. Thus, the subtle structure of the azobenzene chromophore moieties in polymers could be further adjusted to modify the NLO properties of the final yielded materials through polymer reactions. Thus, the present examples might provide some useful information for the synthesis of other functional polymers inaccessible from their monomers. The obtained polyurethanes, especially **P5**, could be good candidates for the practical applications in NLO field.

Acknowledgements

We are grateful to the National Science Foundation of China (no. 20402011 and 20674059), the National Fundamental Key Research Program and Hubei Province for financial support.

References

[1] Ichimura K. Photoalignment of liquid-crystal systems. Chemical Reviews 2000;100:1847–73.
[2] Ikeda T, Tsutsumi O. Optical switching and image storage by means of azobenzene liquid-crystal films. Science 1995;268:1873–5.
[3] Gibbons WM, Shannon PJ, Sun ST, Swetlin BJ. Surface-mediated alignment of nematic liquid crystals with polarized laser light. Nature 1991;351:49–50.
[4] Wang GJ, Wang XG. A novel hyperbranched polyester functionalized with azo chromophore: synthesis and photoresponsive properties. Polymer Bulletin 2002;49:1–8.
[5] Bahuleyan D, Sreekumar K. Chiral polyesters with azobenzene moieties in the main chain, synthesis and evaluation of nonlinear optical properties. Journal of Materials Chemistry 1999;9:1425–9.
[6] Lucchetti L, Simoni F, Reznikov Y. Fast optical recording in dye-doped liquid crystals. Optics Letters 1999;24:1062–4.
[7] Zyss J, editor. Molecular nonlinear optics: materials, physics and devices. New York: Academic Press; 1994.
[8] Barclay GG, Ober CK. Liquid crystalline and rigid-rod networks. Progress in Polymer Science 1993;18:899–945.
[9] Moerner WE, Jepsen AG, Thompson CL. Photorefractive polymers. Annual Review of Materials Science 1997;27:585–623.
[10] Morikawa Y, Nagano S, Watanabe K, Kamata K, Iyoda T, Seki T. Optical alignment and patterning of nanoscale microdomains in a block copolymer thin film. Advanced Materials 2006;18:883–6.
[11] Yu H, Iyoda T, Ikeda T. Photoinduced alignment of nanocylinders by supramolecular cooperative motions. Journal of American Chemical Society 2006;128:11010–1.
[12] Pham VP, Manivannan G, Lessard RA, Bornengo G, Po R. New azo-dye-doped polymer systems as dynamic holographic recording media. Applied Physics A: Materials Science and Processing 1995;60:239–42.
[13] Lagugne-Labarthet F, Buffeteau T, Sourisseau C. Inscription of holographic gratings using circularly polarized light: influence of the optical set-up on the birefringence and surface relief grating properties. Applied Physics B: Lasers and Optics 2002;74:129–37.
[14] Lefin P, Fiorini C, Nunzi JM. Anisotropy of the photo-induced translation diffusion of azobenzene dyes in polymer matrices. Pure and Applied Optics 1998;7:71–82.
[15] Marder SR, Cheng LT, Tiemann BG, Friedli AC, Blanchard-Desce M, Perry JW, et al. Large first hyperpolarizabilities in push–pull polyenes by tuning of the bond length alternation and aromaticity. Science 1994;263:511–4.
[16] Luo J, Ma H, Haller M, Barto RR. Large electro-optic activity and low optical loss derived from a highly fluorinated dendritic nonlinear optical chromophore. Chemical Communications 2002:888–9.

[17] Yang S, Li L, Cholli AL, Kumar J, Tripathy SK. Photoinduced surface relief gratings on azocellulose films. Journal of Macromolecular Science A: Pure and Applied Chemistry 2001;38:1345–54.
[18] Xu ZS, Drnoyan V, Natansohn A, Rochon A, Rochon R. Novel polyesters with amino-sulfone azobenzene chromophores in the main chain. Journal of Polymer Science, Part A: Polymer Chemistry 2000;38:2245–53.
[19] Gubbelmans E, Verbiest T, Van Beylen M, Persoons A, Samyn C. Chromophore-functionalised polymides with high-poling stabilities of the nonlinear optical effect at elevated temperature. Polymer 2002;43:1581–5.
[20] Angiolini L, Caretti D, Giorgini L, Salatelli E. Synthesis and chiroptical properties of optically active photochromic methacrylic polymers bearing in the side chain the (*S*)-3-hydroxypyrrolidinyl group conjugated with the *trans*-azoaromatic chromophore. Journal of Polymer Science, Part A: Polymer Chemistry 1999;37:3257–68.
[21] Li N, Xu Q, Lu J, Xia X, Wang L. Atom transfer radical polymerization and third-order nonlinear optical properties of new azobenzene-containing side-chain polymers. Macromolecular Chemistry and Physics 2007;208:399–404.
[22] Liu L, Nakatani K, Pansu R, Vachon JJ, Tauc P, Ishow E. Fluorescence patterning through photoinduced migration of squaraine-functionalized azo derivatives. Advanced Materials 2007;19:433–6.
[23] Wang Q, Wang LM, Yu LP. Development of fully functionalized photorefractive polymers. Macromolecular Rapid Communications 2000;21:723–45.
[24] Wang X, Kumar J, Tripathy SK, Li L, Chen JI, Marturunkakul S. Epoxy-based nonlinear optical polymers from post azo coupling reaction. Macromolecules 1997;30:219–25.
[25] Li Z, Qin J, Tang H, Liu Y. Postfunctionalization strategy for developing polyphosphazene with a high loading of highly polar molecules in the side arms. Journal of Applied Polymer Science 2003;89:2989–93.
[26] Li Z, Qin J, Li S, Ye C. Second-order nonlinear optical property of polysiloxane containing indole-based multifunctional chromophore. Synthetic Metals 2003;135:467–8.
[27] Li Z, Li J, Qin J, Qin A, Ye C. Synthesis and characterization of polysiloxanes containing carbazolyl and sulfonyl-indole based chromophore as side chains. Polymer 2005;46:363–8.
[28] Li Z, Gong W, Qin J, Yang Z, Ye C. Second-order nonlinear optical property of polyphosphazenes containing charge-transporting agents and indole-based chromophore. Polymer 2005;46:4971–8.
[29] Fréchet JMJ, Hawker CJ, Gitsov I, Leon JW. Dendrimers and hyperbranched polymers: two families of three-dimensional macromolecules with similar but clearly distinct properties. Journal of Macromolecular Science A: Pure and Applied Chemistry 1996;A33:1399–425.
[30] Hecht S, Fréchet JMJ. Dendritic encapsulation of function: applying nature's site isolation principle from biomimetics to materials science. Angewandte Chemie International Edition 2001;40:74–91.
[31] Pereverzev YV, Prezhdo OV, Dalton LR. Macroscopic order and electro-optic response of dipolar chromophore–polymer materials. ChemPhysChem 2004;5:1821–30.
[32] Robinson BH, Dalton LR. Monte Carlo statistical mechanical simulations of the competition of intermolecular electrostatic and poling-field interactions in defining macroscopic electro-optic activity for organic chromophore/polymer materials. Journal of Physical Chemistry A 2000;104:4785–95.
[33] Kim TD, Luo J, Tian Y, Ka JW, Tucker NM, Haller M, et al. Diels–Alder "click chemistry" for highly efficient electrooptic polymers. Macromolecules 2006;39:1676–80.
[34] Ma H, Liu S, Luo J, Suresh S, Liu L, Kang SH, et al. Highly efficient and thermally stable electro-optical dendrimers for photonics. Advanced Functional Materials 2002;12:565–74.
[35] Ma H, Chen BQ, Sassa T, Dalton LR, Jen AKY. Highly efficient and thermally stable nonlinear optical dendrimer for electrooptics. Journal of American Chemical Society 2001;123:986–7.
[36] Bai Y, Song N, Gao JP, Sun X, Wang X, Yu G, et al. A new approach to highly electrooptically active materials using cross-linkable, hyperbranched chromophore-containing oligomers as a macromolecular dopant. Journal of American Chemical Society 2005;127:2060–1.
[37] Li Z, Qin J, Li S, Ye C, Luo J, Cao Y. Polyphophazene containing indole-based dual chromophores: synthesis and nonlinear optical characterization. Macromolecules 2002;35:9232–5.
[38] Li Z, Huang C, Hua J, Qin J, Yang Z, Ye C. A new postfunctional approach to prepare second-order nonlinear optical polyphophazenes containing sulfonyl-based chromophore. Macromolecules 2004;37:371–6.
[39] Tian Y, Zhang X, Wu J, Fun H, Jiang M, Xu Z, et al. Structural diversity and properties of a series of dinuclear and mononuclear copper(II)and copper(I)carboxylato complexes. New Journal of Chemistry 2002;26:1468–73.
[40] Woo HY, Shim HK, Lee KS. Synthesis and optical properties of polyurethanes containing a highly NLO active chromophore. Macromolecular Chemistry and Physics 1998;199:1427–33.
[41] Park CK, Zieba J, Zhao CF, Swedek B, Wijekoon WMEP, Prasad PN. Highly cross-linked polyurethane with enhanced stability of second-order nonlinear optical properties. Macromolecules 1995;28:3713–7.
[42] Lee JY, Bang HB, Park EJ, Lee WJ, Rhee BK, Lee SM. Synthesis and electro-optical properties of novel Y-type polyurethanes containing dioxynitrostilbene. Polymer International 2004;53:1838–44.
[43] Hiroya K, Matsumoto S, Sakamoto T. New synthetic method for indole-2-carboxylate and its application to the total synthesis of duocarmycin SA. Organic Letters 2004;6:2953–6.
[44] Courtin A. Notiz zur synthese von alkyl-, cycloalkyl- und aryl-(4-aminophenyl)-sulfonen. Helvetica Chimica Acta 1983;66:1046–52.
[45] Li Z, Qin A, Lam JWY, Dong Y, Dong Y, Ye C, et al. Facile synthesis, large optical nonlinearity, and excellent thermal stability of hyperbranched poly(aryleneethynylene)s containing azobenzene chromophores. Macromolecules 2006;39:1436–42.
[46] Li Q, Li Z, Zeng F, Gong W, Li Z, Zhu Z, et al. From controllable attached isolation moieties to possibly highly efficient nonlinear optical main-chain polyurethanes containing indole-based chromophores. Journal of Physical Chemistry B 2007;111:508–14.
[47] Li Z, Li Z, Di C, Zhu Z, Li Q, Zeng Q, et al. Structural control of the side-chain chromophores to achieve highly efficient nonlinear optical polyurethanes. Macromolecules 2006;39:6951–61.
[48] Li Z, Zeng Q, Li Z, Dong S, Zhu Z, Li Q, et al. An attempt to modify nonlinear optical effects of polyurethanes by adjusting the structure of the chromophore moieties at molecular level using "click" chemistry. Macromolecules 2006;39:8544–6.
[49] Zeng Q, Li Z, Li Z, Ye C, Qin J, Tang BZ. Convenient attachment of highly polar azo chromophore moieties to disubstituted polyacetylene through polymer reactions by using "click" chemistry. Macromolecules 2007;40:5634–7.
[50] Moylan CR, Miller RD, Twieg RJ, Lee VY, McComb IH, Ermer S, et al. Defeating tradeoffs for nonlinear optical chromophores. Proceedings of SPIE 1995;2527:150–62.